Automatic Wood Pith Detector: Local Orientation Estimation and Robust Accumulation

Henry Marichal, Diego Passarella and Gregory Randall

UNIVERSIDAD DE LA REPÚBLICA URUGUAY

FACULTAD DE INGENIERÍA UDELAR

CENUR Litoral Norte

ANII

ICPR 2024 INDIA

Why is Pith Detection Important?

- Essential for determining the **first year of growth** and estimating **tree age**.
- The pith has distinct physical-mechanical properties, making it critical for:
  - Detecting **growth eccentricity**.
  - Identifying areas prone to **fungal degradation**.
  - Distinguishing wood sections for **industrial applications**.

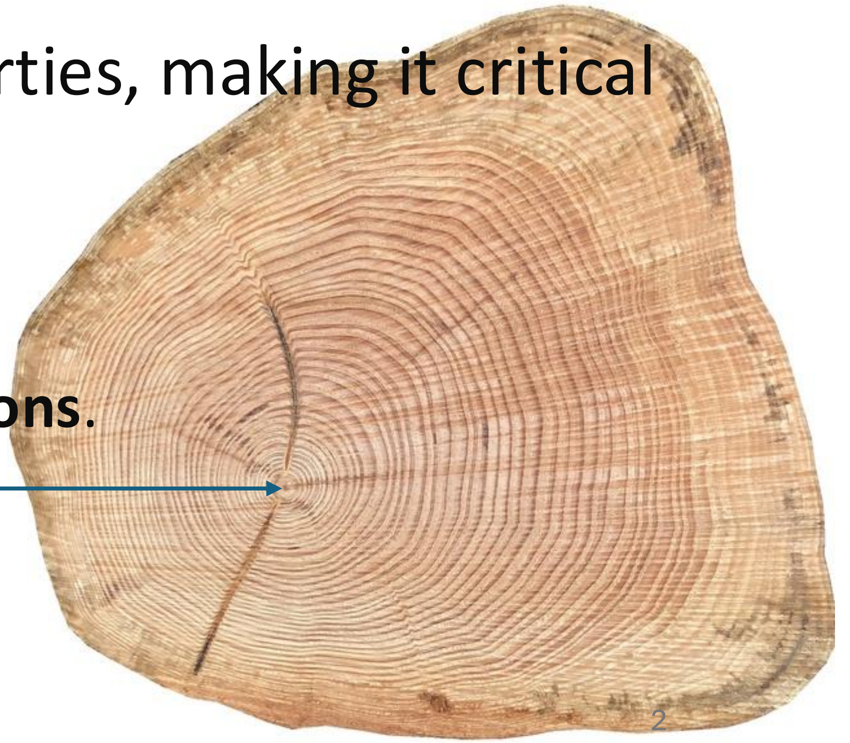

Challenges in Pith Detection

- Natural wood irregularities
    - **Ring asymmetries**, **cracks**, **knots**, and **fungal degradation**.

Challenges by Species

- **Species diversity**
  - Gymnosperms and angiosperms exhibit different wood structures.

Pinus Taeda

Douglas Fir

Gleditsia triacanthos

Automatic Ring Detection

- Automatic Tree Ring delineation algorithms sensitive to precise pith location, especially those relying on the **concentric ring pattern**

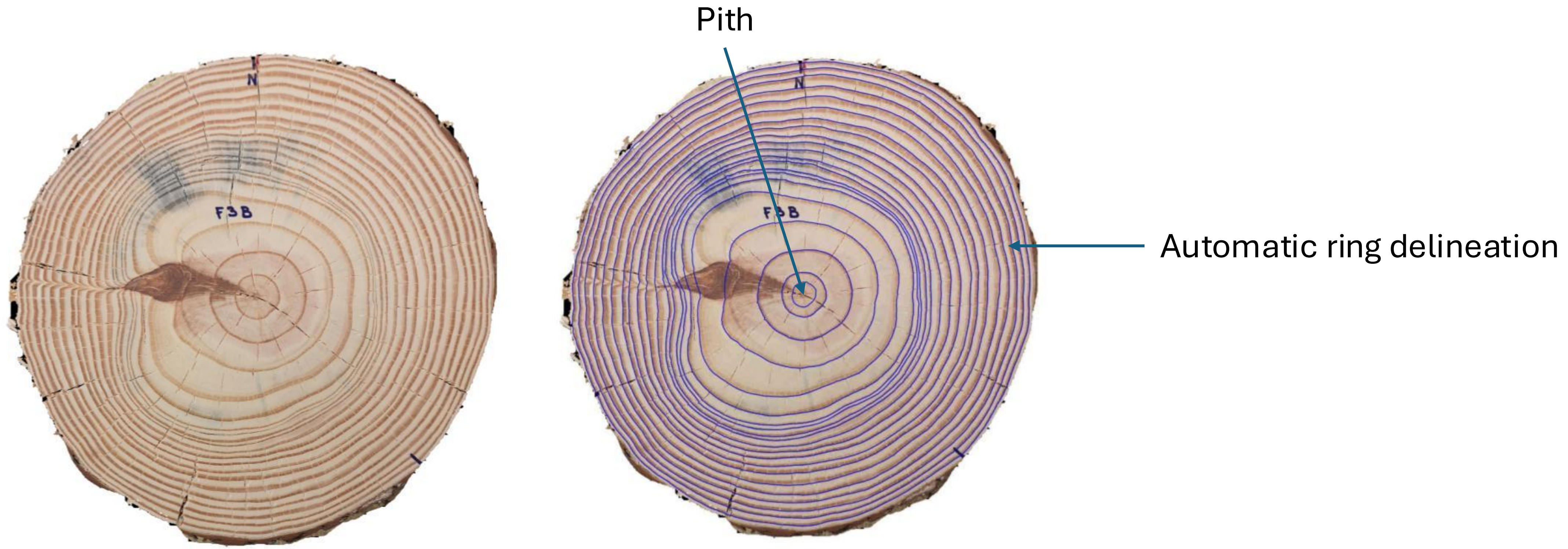

CS-TRD: a Cross Sections Tree Ring Detection method

Iterative Next Boundary Detection for Instance Segmentation of Tree Rings in Microscopy Images of Shrub Cross Sections

Objective

- Develop automated, reliable method for pith detection that handle variability across species, conditions, and structural irregularities.



Tree Disk Structure

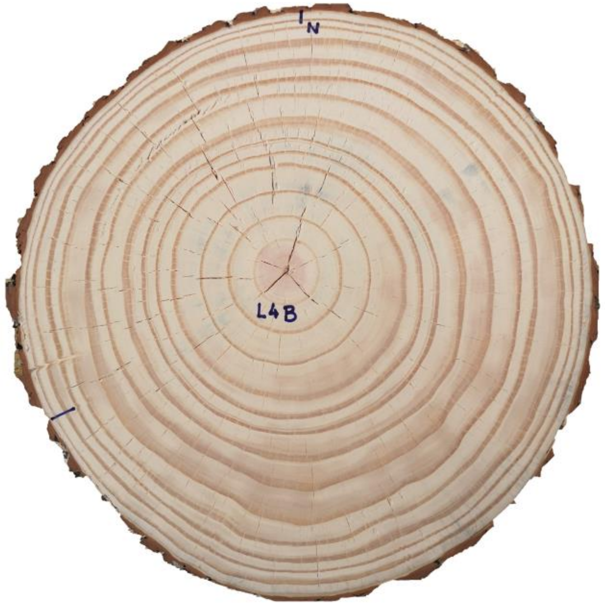

Tree disk model

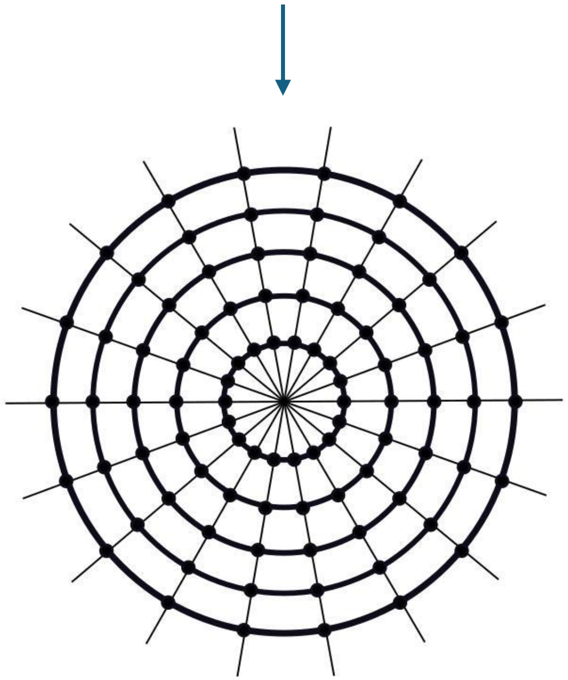

- Two main structures
  - Tree Rings formed by roughly concentric curves
  - Radial structures such as cracks and fungi

- Intersection of the lines supported by radial structures and the perpendicular to the rings is close to the pith

Computing Ring Normals

- Local orientation (LO) estimation at each pixel
  - 2D-Structure Tensor
- Splitting the image is patches, we assign to each patch the local orientation with highest coherence
- Some LOs are going to be noise

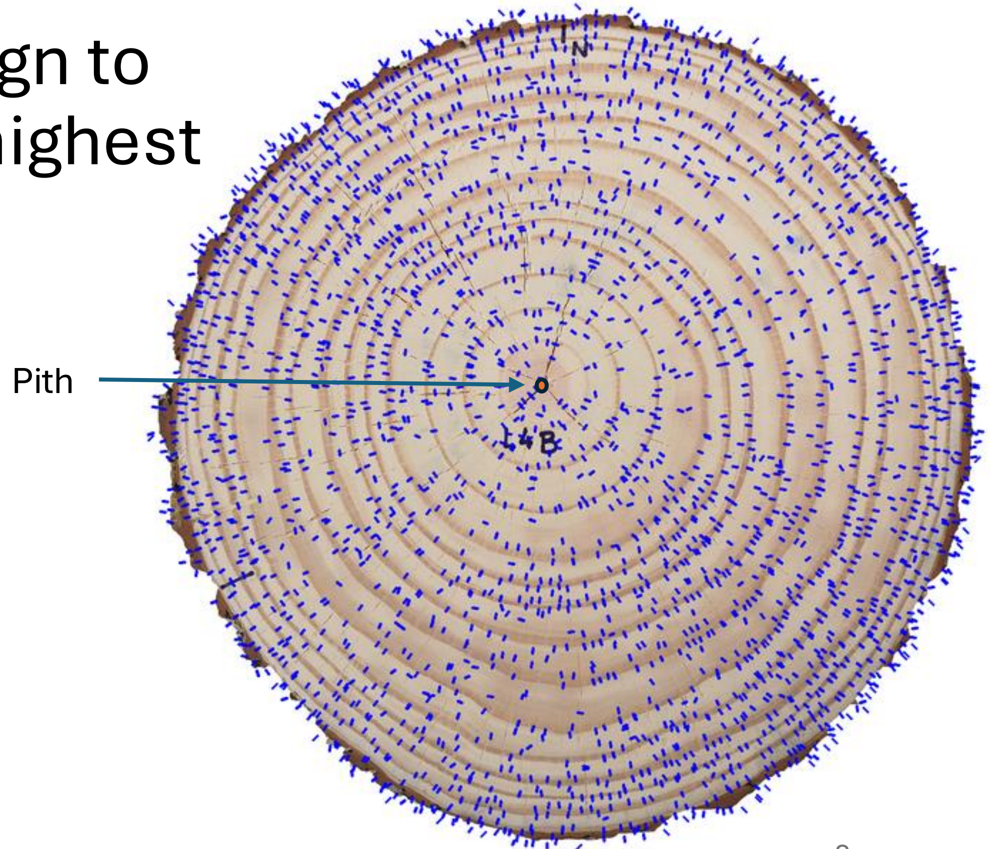

Sampled LO

Accumulation Space

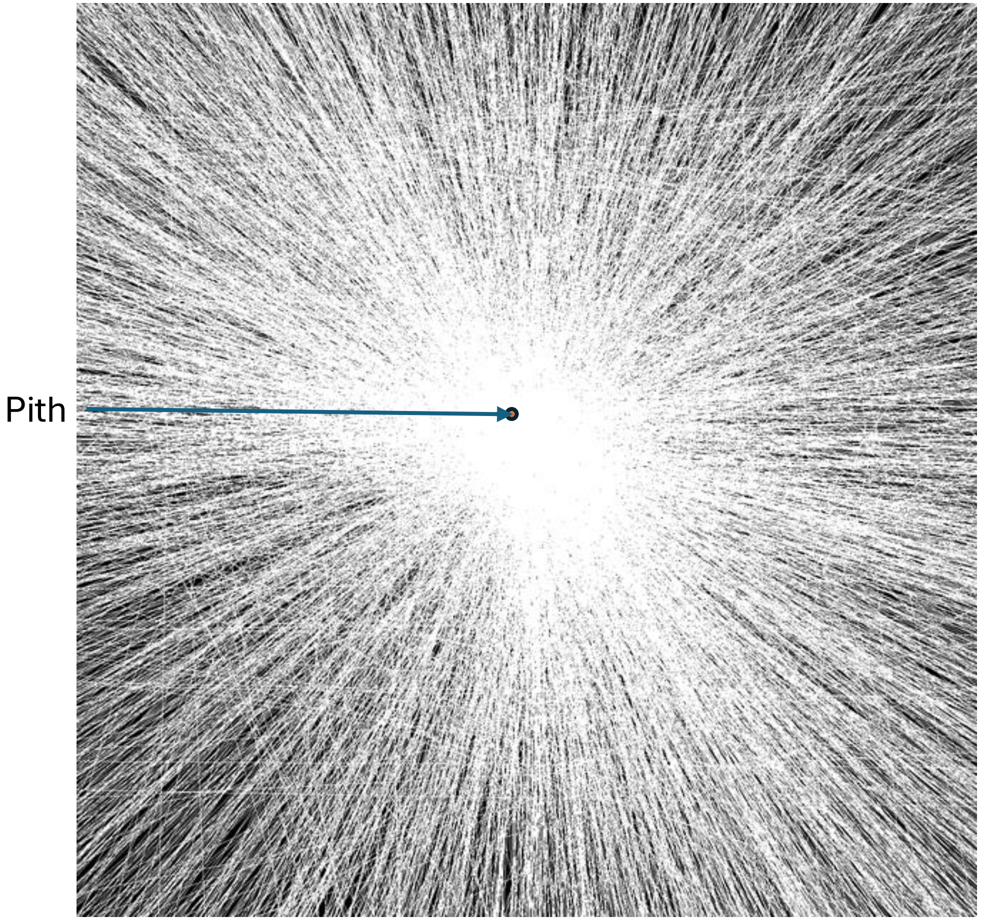

- Accumulating the LOs we can see how the pith region is highlighted.
- In order to have an accurate pith localization we need a way of accumulate them intelligently.
  - Removing LO that does not belong to the ring structure

Alignment-Based Detection

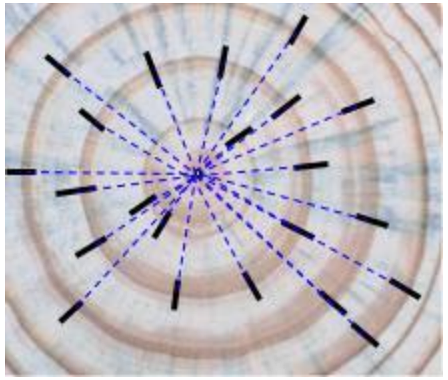

Fig1

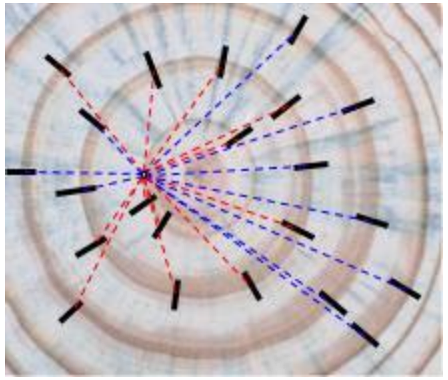

Fig2

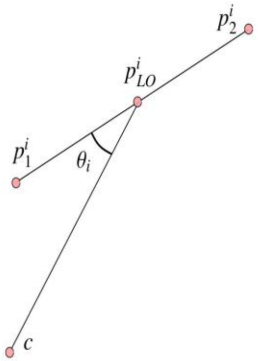

Pith candidate at iteration n

Fig3

- Intuitively the angle (Θ_i) between the pith position and the pixel belonging to the ring (p_{LO}^i) and **LO** $p_1^i p_2^i$ should be close to 0 (or 180).
  - If Θ_i is close to 0, $cos^2(\Theta_i)$ is close to 1.
- $h(x, y) = \frac{1}{N} \sum_{i=1}^{N} cos^2(\Theta_i(x, y))$

$$\cos(\theta_i(x,y)) = \frac{<\overline{cp^i_{LO}}, \overline{p^i_1 p^i_2}>}{|\overline{cp^i_{LO}}||\overline{p^i_1 p^i_2}|}$$

Refinement Process

h(x,y) peak

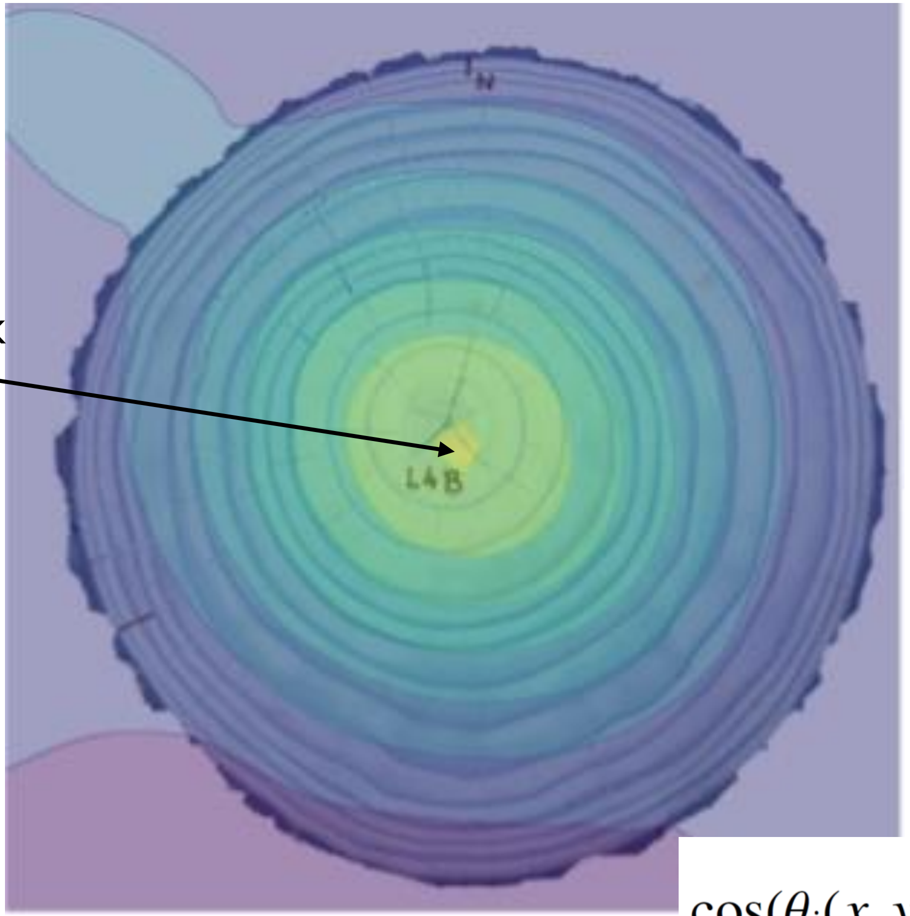

Fig1 h(x,y) level curves

$$h(x,y) = \frac{1}{N}\sum_{i=1}^{N} cos^2(\Theta_i(x,y))$$

- Pith candidate

$$c_{opt} = \max_{c} \quad \frac{1}{N}\sum_{i=1}^{N}\left(\frac{<\overline{cp^i_{LO}}, \overline{p^i_1 p^i_2}>}{|\overline{cp^i_{LO}}||\overline{p^i_1 p^i_2}|}\right)^2$$

$$\text{s.t.} \quad c \in Slice\ Region$$

$$\cos(\theta_i(x,y)) = \frac{<\overline{cp^i_{LO}}, \overline{p^i_1 p^i_2}>}{|\overline{cp^i_{LO}}||\overline{p^i_1 p^i_2}|}$$

Iterative Refinement

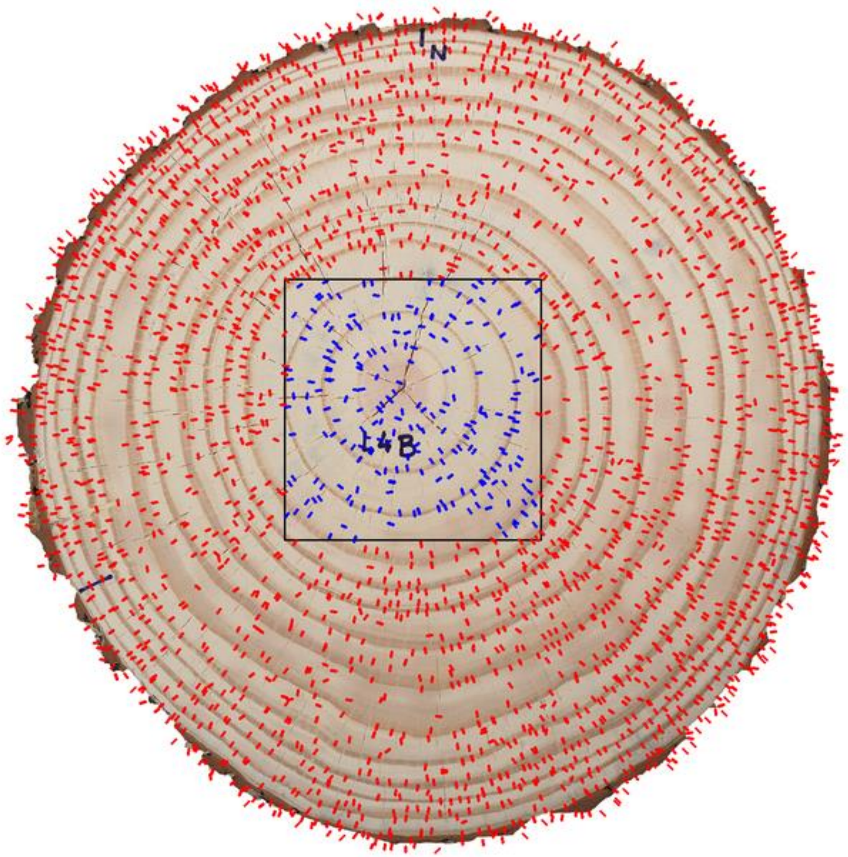

In blue colors is the sub image built around the solution c_1 obtained after the first iteration

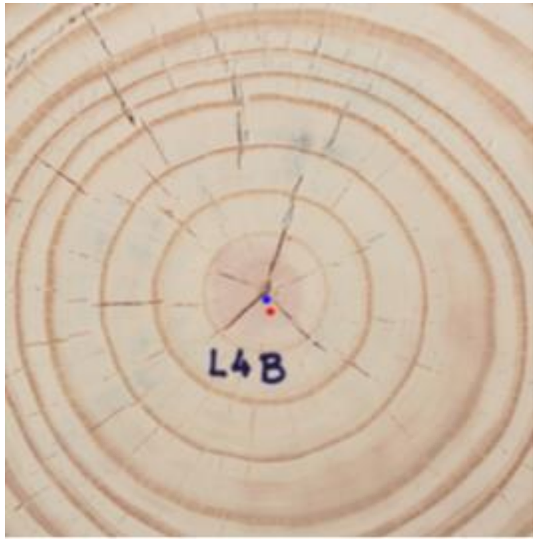

Challenges with Anomalies

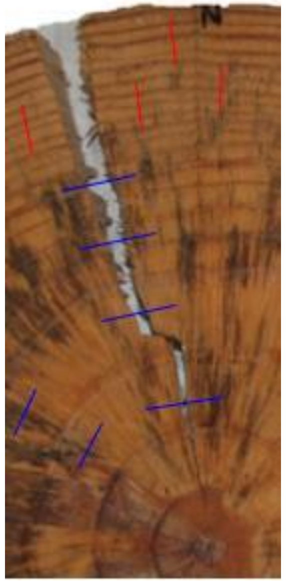

Original LOs

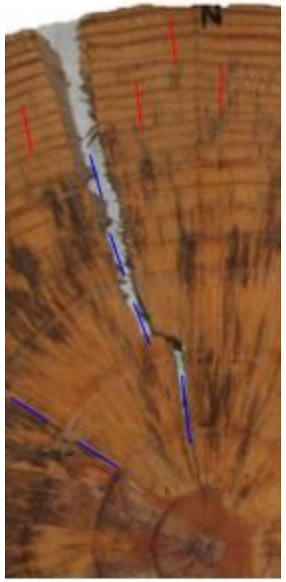

Blue LOs rotated 90 degres

- There are situations where the ring structures not give enough information due to fungi or other perturbations.
- If we can select the LO supported by the radial structures of those perturbations and the normal of the ring structures we could rotate 90 degrees the tangential LOs (blue)

Accumulation Space with Anomalies

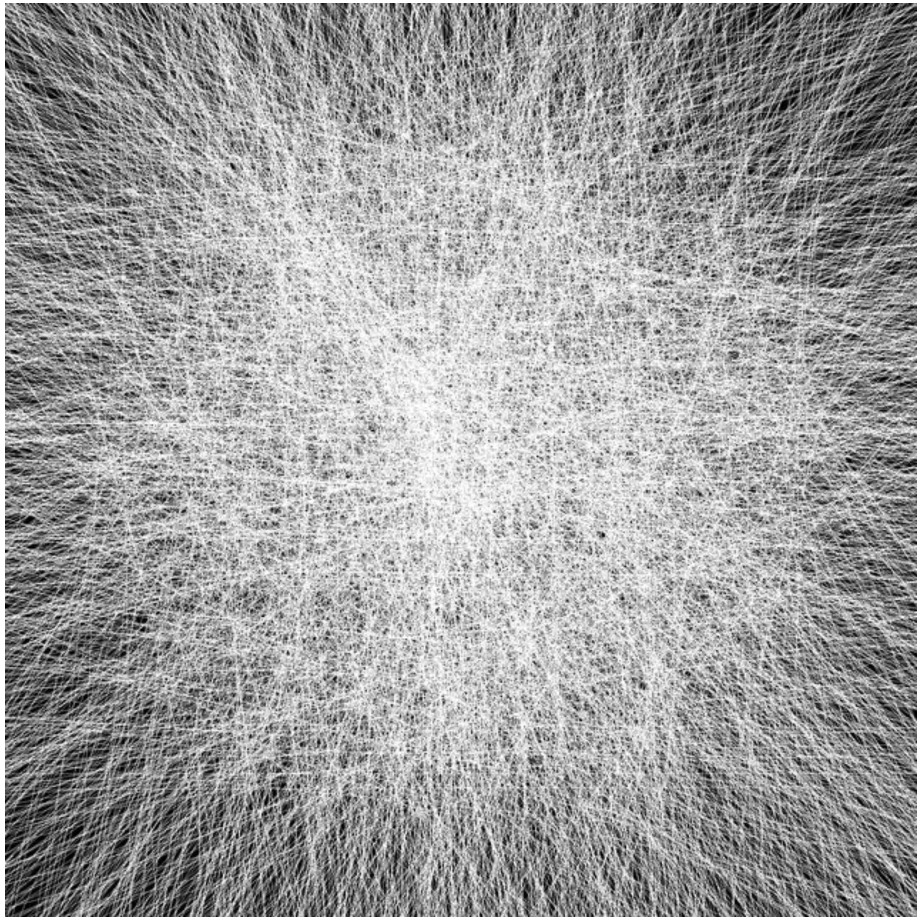

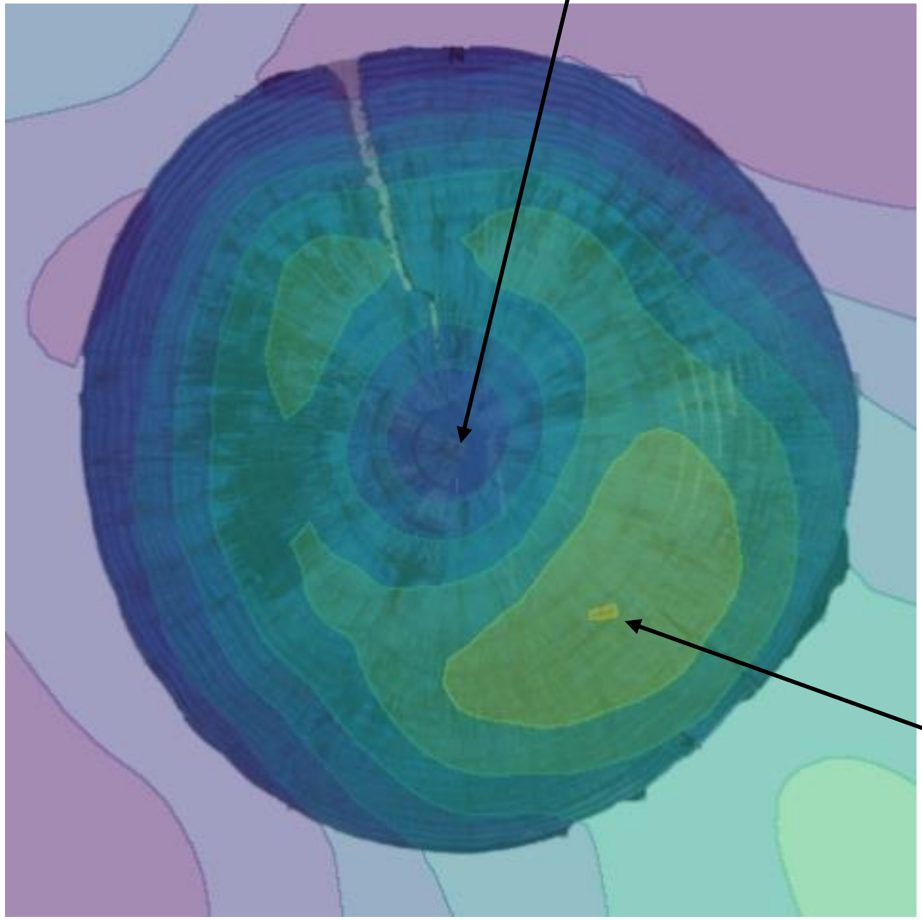

APD Method

Parallel Coordinate Space

- Parallel Coordinate Space,
  - Lines are transformed as dots
  - Converging lines are aligned dots
  - It is composed by two sub-spaces: Twisted and Straight, lines with orientations between 180 and 360 degrees goes to the Twisted, lines with orientation between 0 and 180 degrees goes to the Straight

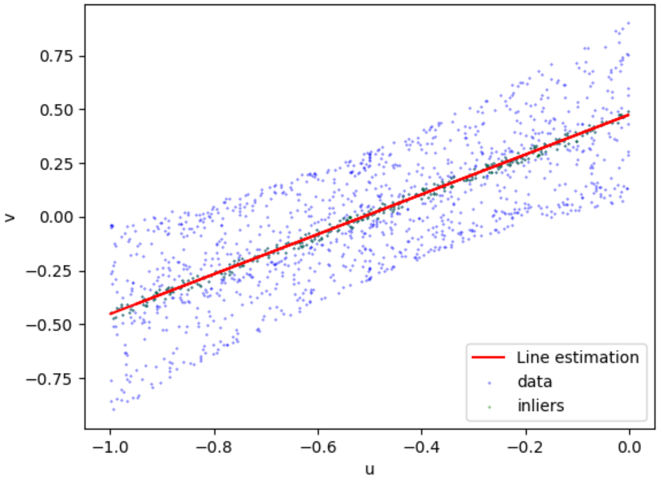

Twisted

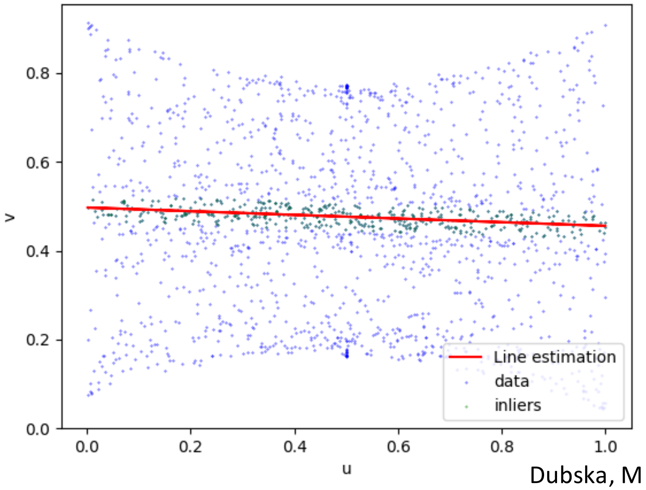

Straight

Aligned lines are selected using Ransac Method

Dubska, M., Herout, A., Havel, J.: Pclines - line detection using parallel coordinates
Fischler, M.A., Bolles, R.C.: Random sample consensus: A paradigm for model fitting with applications to image analysis and automated cartography

Refined Accumulation Space

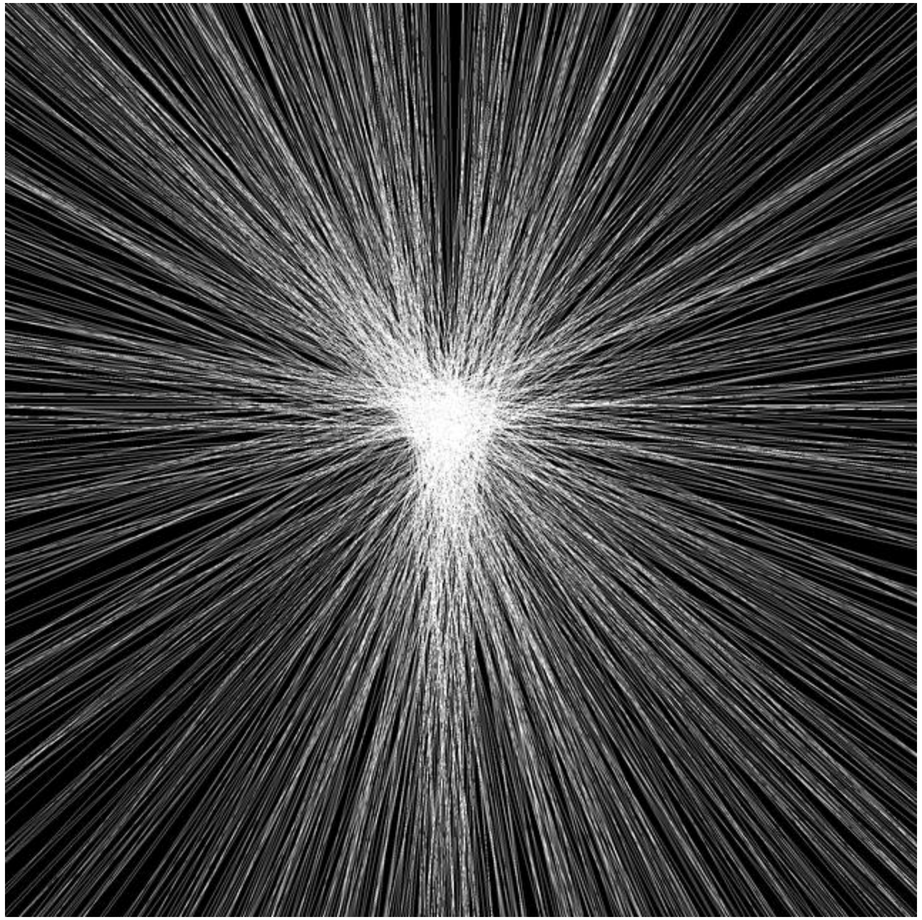

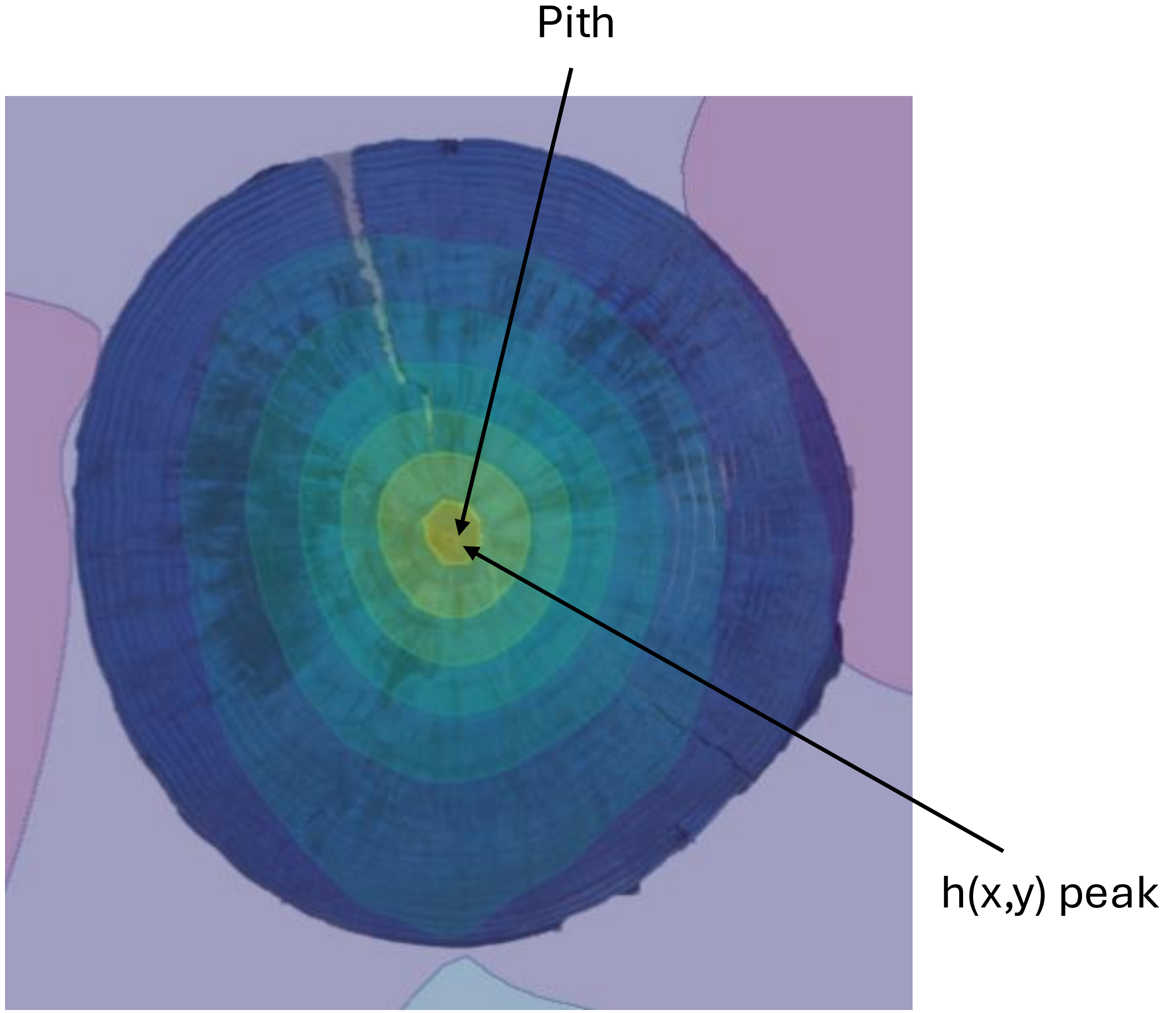

Deep Learning Approach: APD-DL

- **YoloV8 Network**
  - Architecture designed for object detection and segmentation.
  - Inspired by Kurdthongmee et al. (2019, YoloV3).
  - Dataset: Wood cross-section images labeled with pith location as bounding boxes (1/10th of image dimensions).

- **Training & Validation**
  - **Five-Fold Cross-Validation**:
    - Divide data into five subsets.
    - Train on 4 subsets, test on 1
    - Rotate subsets, ensuring no overlap between training and testing data.

Datasets

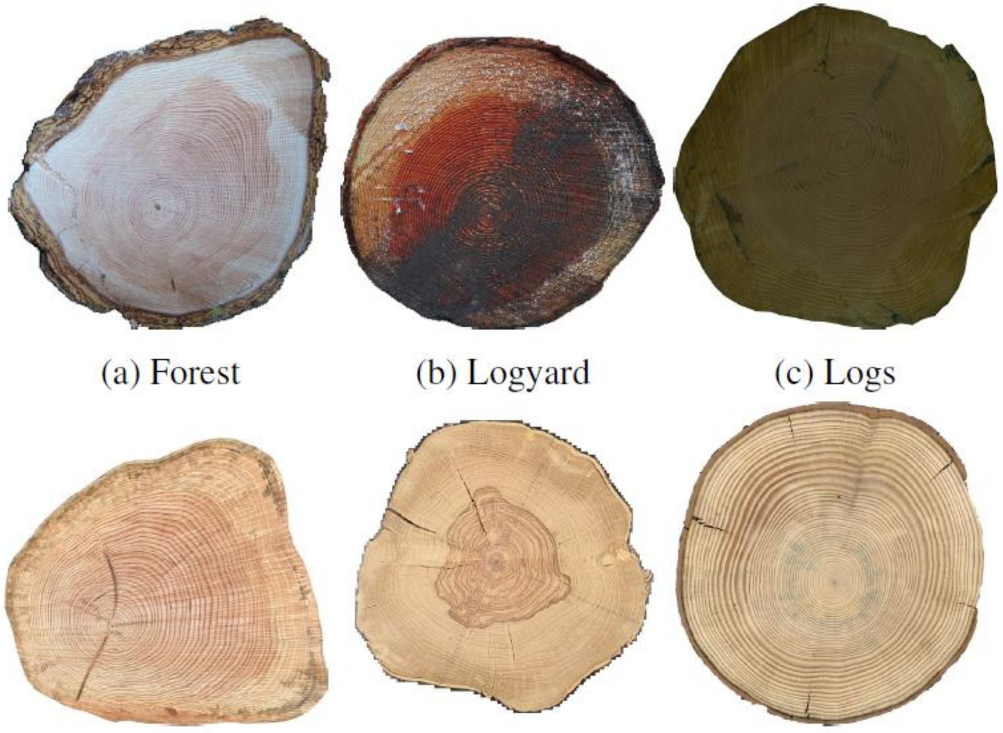

(a) Forest (b) Logyard (c) Logs

(d) Disc (e) UruDendro3 (f) Kennel

Collection	Number of images	Specie
UruDendro2	119	*Pinus taeda*
UruDendro3	9	*Gleditsia triacanthos*
Kennel	7	*Abies alba*
Forest	57	*Douglas fir*
Logyard	32	*Douglas fir*
Logs	150	*Douglas fir*
Discs	208	*Douglas fir*

582

Results

Average over each dataset

Lower the better

	UruDendro2	UruDendro3	Kennel	Forest	Logyard	Logs	Discs
LFSA (21)	1.03 (0.85)	1.46 (0.97)	0.42 (0.18)	0.80 (0.36)	1.02 (0.62)	0.80 (0.46)	0.72 (0.43)
ACO (3)	2.23 (6.64)	4.52 (11.96)	0.2 (0.06)	0.24 (0.24)	0.60 (1.11)	0.46 (0.45)	0.24 (0.35)
APD-PCL	**0.42 (0.34)**	0.74 (0.54)	0.19 (0.10)	0.81 (0.98)	0.82 (0.84)	0.52 (0.47)	0.46 (0.57)
APD	1.02 (2.45)	0.55 (0.30)	**0.14 (0.06)**	**0.22 (0.18)**	**0.35 (0.17)**	0.29 (0.33)	0.26 (0.42)
APD-DL	0.55 (1.45)	**0.13 (0.06)**	0.14 (0.07)	0.45 (1.85)	0.52 (1.29)	**0.22 (0.46)**	**0.23 (0.54)**

Results on all the datasets. Normalized errors. We show the mean error and the standard deviation between parenthesis.

(3) Decelle, R., Ngo, P., Debled-Rennesson, I., Mothe, F., Longuetaud, F.: Ant Colony Optimization for Estimating Pith Position on Images of Tree Log Ends.
(21) Schraml, R., Uhl, A.: Pith estimation on rough log end images using local fourier spectrum analysis.

Performance Summary

Average over the full dataset (582 samples)

Lower the better

Method	Mean	Median	Max	FN	Time
LFSA (21)	0.83	0.72	5.03	0	627
ACO (3)	0.79	0.21	36.39	2	918
APD-PCL	0.52	0.34	4.33	0	2339
APD	0.42	0.19	15.44	0	784
APD-DL	0.33	0.14	13.91	3	209

Results of all the methods over the whole set of images, i.e., merging all collections. Normalized errors, number of false negatives, and execution time in milliseconds.

(3) Decelle, R., Ngo, P., Debled-Rennesson, I., Mothe, F., Longuetaud, F.: Ant Colony Optimization for Estimating Pith Position on Images of Tree Log Ends.
(21) Schraml, R., Uhl, A.: Pith estimation on rough log end images using local fourier spectrum analysis.

Qualitative results

Purple, LFSA; Red, ACO; Blue, APD; Yellow, APD-PCL and Green, APD-DL

Sample with fungal degradation. APD-PCL is the best method

Qualitative results

Purple, LFSA; Red, ACO; Blue, APD; Yellow, APD-PCL and Green, APD-DL

Sample with fungal degradation. APD-PCL is the best method

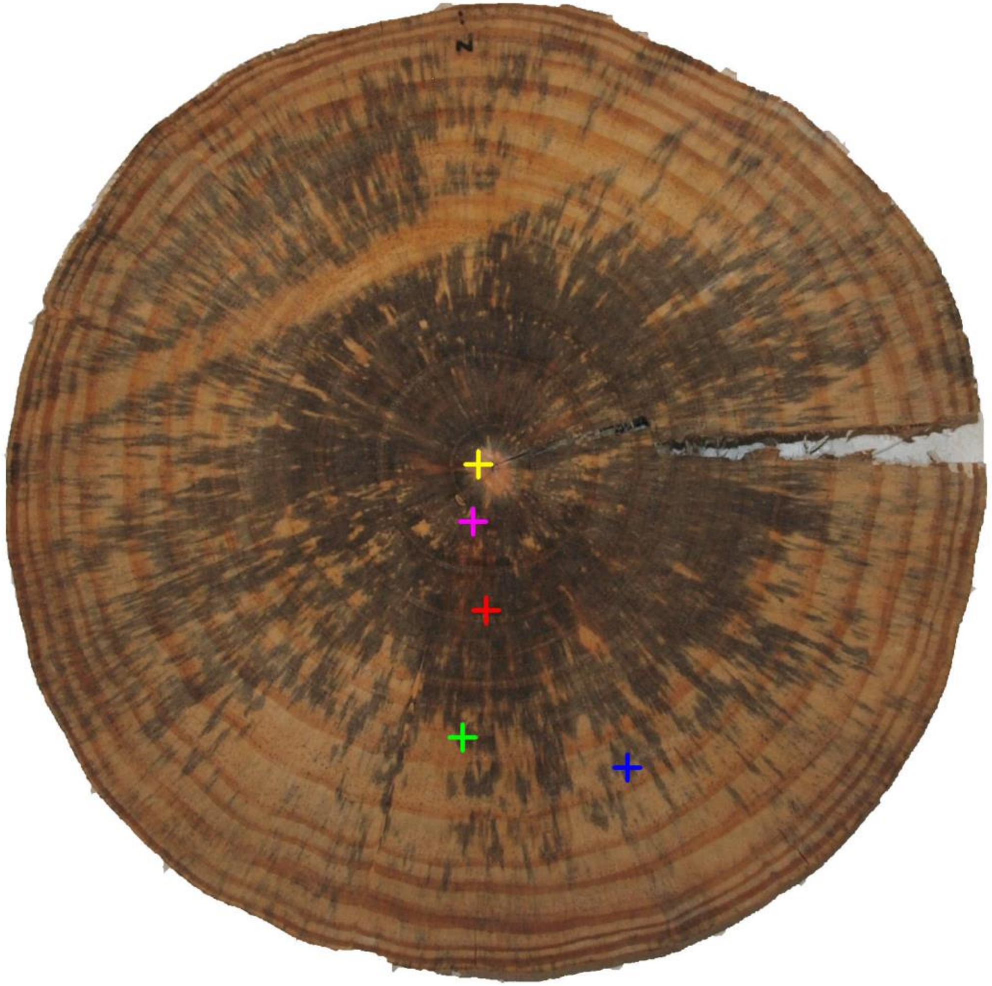

Qualitative results

Purple, LFSA; Red, ACO; Blue, APD; Yellow, APD-PCL and Green, APD-DL

Sample with fungal degradation. APD-PCL is the best method

Conclusions

- Proposed a comparative study of classic and machine learning-based methods for pith detection.
- Introduced the **UruDendro Dataset**, enhancing the community’s ability to benchmark and develop new methods.
- Methods were assessed over different species, acquisitions condition and perturbations.
- APD method outperformed the YoloV8 model in the datasets Kennel, Forest and Logyard

Thanks

henry.marichal@fing.edu.uy

UNIVERSIDAD DE LA REPÚBLICA URUGUAY

FACULTAD DE INGENIERÍA UDELAR

CENUR Litoral Norte

ANII

ICPR 2024 INDIA